Tenth International Conference on Computational Fluid Dynamics (ICCFD10), Barcelona, Spain, July 9-13, 2018

ICCFD10-0401

A Cell-Centered Finite Volume Based Hyperbolic Method for Incompressible Navier-Stokes Equations on Unstructured Grids

D. Kim* and H. T. Ahn*
Corresponding author: htahn@ulsan.ac.kr

*School of Naval Architecture and Ocean Engineering, University of Ulsan, Ulsan, Korea

1 Introduction

Standard finite volume method based on linear solution reconstruction is considered as second order accurate for solution variables, i.e. pressure and velocity components[1]. The second order accuracy is based on the second order accurate evaluation of the convective flux. However for the computation of viscous flux involving solution derivatives, for example the velocity gradients, is merely first order accurate on general unstructured grids and easily to be degraded from the nominal order of accuracy where mesh regularity is poor. The issue related to the viscous flux computation persists, even for more advanced spatial discretization methods, e.g. discontinuous Galerkin or high-order solution reconstruction, due to possible inconsistency in viscous flux computation[2]. Recently, a very new, efficient, and accurate method is proposed by Nishikawa[4,5], and its applicability towards three-dimensional realistic problem is presented by Nishikawa and his co-workers[6]. Also, high-order reconstruction based finite volume method for hyperbolic diffusion system is presented[7]. This method is based on the re-formulation of elliptic nature of the viscous fluxes into a set of augmented variables than makes the entire system to be hyperbolic. In this paper, a hyperbolic incompressible Navier-Stokes (Hyper-INS) system is presented and the solution is obtained by cell-centered finite volume method using unstructured meshes[8]. A very promising result, the uniform order of accuracy not only for the solution variables but also for their gradients are obtainable, will be presented. An even more efficient scheme, so called a hybrid scheme (or scheme II) which utilizing the gradient variables for solution variable reconstruction, is also presented and its superior accuracy is demonstrated.

2 Hyperbolic incompressible Navier-Stokes formulation

Based on the artificial compressibility formulation [1,3] of non-dimensionalized Navier-Stokes equations for incompressible flows, the hyperbolic formulation, originally proposed by Nishikawa[4,5,6], can be presented in a differential form as follows,

$$\frac{\partial}{\partial t}Q + \nabla \cdot \boldsymbol{F} = \mathrm{S}.$$

In two spatial dimensions, the divergence term can be expressed as follows,

$$\frac{\partial}{\partial t}Q + \frac{\partial}{\partial x}F + \frac{\partial}{\partial y}G = \mathrm{S}.$$

And the each component can be expressed as follows,

$$Q=\begin{Bmatrix} p\\ u\\ v\\ u_x\\ u_y\\ v_x\\ v_y \end{Bmatrix},\; F=\begin{Bmatrix} \beta u\\ (uu+p)-\left(\frac{1}{Re}u_x\right)\\ (vu)-\left(\frac{1}{Re}v_x\right)\\ -\frac{u}{T_r}\\ 0\\ -\frac{v}{T_r}\\ 0 \end{Bmatrix},\; G=\begin{Bmatrix} \beta v\\ (uv)-\left(\frac{1}{Re}u_y\right)\\ (vv+p)-\left(\frac{1}{Re}v_y\right)\\ 0\\ -\frac{u}{T_r}\\ 0\\ -\frac{v}{T_r} \end{Bmatrix},\; S=\begin{Bmatrix} 0\\ 0\\ 0\\ -\frac{u_x}{T_r}\\ -\frac{u_y}{T_r}\\ -\frac{v_x}{T_r}\\ -\frac{v_y}{T_r} \end{Bmatrix}.$$

Here the state vector Q contains both the solution varialbes (p,u,v) and the gradient variables (u_x,u_y,v_x,v_y). β is the artificial compressibility parameter and T_r is the relaxation time scale introduced by the hyperbolic formulation, and Re is Reynolds number.
The above differential form can be expressed in an integral form over a closed control volume Ω as follows,

$$\frac{\mathrm{d}}{\mathrm{dt}}\int_{\Omega} Q dV + \oint_{\partial\Omega} (F\cdot n) dS = \int_{\Omega} S dV$$

where the vector of cell-averaged state variables, the flux vector, and source term on the right hand side are defined as follows.

$$Q=\begin{Bmatrix} p\\ u\\ v\\ u_x\\ u_y\\ v_x\\ v_y \end{Bmatrix},(\mathrm{F}\cdot\mathrm{n})=\begin{Bmatrix} \beta(un_x+vn_y)\\ (uu+p)n_x+(uv)n_y-\frac{1}{Re}(u_xn_x+u_yn_y)\\ (\mathrm{vu})n_x+(vv+p)n_y-\frac{1}{Re}(v_xn_x+v_yn_y)\\ -\frac{u}{T_r}n_x\\ -\frac{u}{T_r}n_y\\ -\frac{v}{T_r}n_x\\ -\frac{v}{T_r}n_y \end{Bmatrix},S=\begin{Bmatrix} 0\\ 0\\ 0\\ -\frac{u_x}{T_r}\\ -\frac{u_y}{T_r}\\ -\frac{v_x}{T_r}\\ -\frac{v_y}{T_r} \end{Bmatrix}$$

By following the name convection of Nishikawa, the above system of equation can be term as HINS7, which is the basic formulation for the current paper.
For the actual computation of flux term, it is decomposed into two parts, namely convective flux and viscous flux

$$
\boldsymbol{F}_{conv}^{HiNS}+\boldsymbol{F}_{visc}^{HiNS}=\begin{Bmatrix} \beta\left(un_x+vn_y\right) \\ (uu+p)n_x+(uv)n_y \\ (vu)n_x+(vv+p)n_y \\ 0 \\ 0 \\ 0 \\ 0 \end{Bmatrix}+\begin{Bmatrix} 0 \\ -\frac{1}{Re}\left(u_x n_x+u_y n_y\right) \\ -\frac{1}{Re}\left(v_x n_x+v_y n_y\right) \\ -\frac{u}{T_r}n_x \\ -\frac{u}{T_r}n_y \\ -\frac{v}{T_r}n_x \\ -\frac{v}{T_r}n_y \end{Bmatrix}
$$

And each of the flux terms are computed by upwind scheme based on the Eigen decomposition of the flux Jacobian matrices,

$$
\boldsymbol{A}_{Conv}^{HiNS}=\frac{\boldsymbol{\partial}}{\boldsymbol{\partial Q}}\boldsymbol{F}_{conv}^{HiNS}=\frac{\boldsymbol{\partial}}{\boldsymbol{\partial Q}}\begin{Bmatrix} \beta\left(un_x+vn_y\right) \\ (uu+p)n_x+(uv)n_y \\ (vu)n_x+(vv+p)n_y \\ 0 \\ 0 \\ 0 \\ 0 \end{Bmatrix}=\begin{bmatrix} 0 & \beta n_x & \beta n_y & 0 & 0 & 0 & 0 \\ n_x & \theta+un_x & un_y & 0 & 0 & 0 & 0 \\ n_y & vn_x & \theta+vn_y & 0 & 0 & 0 & 0 \\ 0 & 0 & 0 & 0 & 0 & 0 & 0 \\ 0 & 0 & 0 & 0 & 0 & 0 & 0 \\ 0 & 0 & 0 & 0 & 0 & 0 & 0 \\ 0 & 0 & 0 & 0 & 0 & 0 & 0 \end{bmatrix}
$$

$$
\boldsymbol{A}_{visc}^{HiNS}=\frac{\boldsymbol{\partial}}{\boldsymbol{\partial Q}}\boldsymbol{F}_{visc}^{HiNS}=\frac{\boldsymbol{\partial}}{\boldsymbol{\partial Q}}\begin{Bmatrix} 0 \\ -\frac{1}{Re}\left(u_x n_x+u_y n_y\right) \\ -\frac{1}{Re}\left(v_x n_x+v_y n_y\right) \\ -\frac{u}{T_r}n_x \\ -\frac{u}{T_r}n_y \\ -\frac{v}{T_r}n_x \\ -\frac{v}{T_r}n_y \end{Bmatrix}=\begin{bmatrix} 0 & 0 & 0 & 0 & 0 & 0 & 0 \\ 0 & 0 & 0 & -\frac{n_x}{Re} & -\frac{n_y}{Re} & 0 & 0 \\ 0 & 0 & 0 & 0 & 0 & -\frac{n_x}{Re} & -\frac{n_y}{Re} \\ 0 & -\frac{n_x}{T_r} & 0 & 0 & 0 & 0 & 0 \\ 0 & -\frac{n_y}{T_r} & 0 & 0 & 0 & 0 & 0 \\ 0 & 0 & -\frac{n_x}{T_r} & 0 & 0 & 0 & 0 \\ 0 & 0 & -\frac{n_y}{T_r} & 0 & 0 & 0 & 0 \end{bmatrix}
$$

Note that the Eigen values of the above flux Jacobians are all real and the system of equation is indeed hyperbolic.

3 Discretization scheme

The integral form of the governing equation can be approximated over the finite volume delineated in Fig.1 as follows. As the solution is approximated by low degree polynomials, either piecewise constant or linear, the spatial integration of the governing equation ca be simplified as follows,

$$
\frac{d}{dt}\left(\bar{Q}_i\Omega_i\right)+\sum_{j=1}^{N_{nei}}F\left(Q_L,Q_R;n_{ij}\right)\cdot\Delta s_{ij}=\bar{S}_i\Omega_i,
$$

where $\bar{Q}_i$ and $\bar{S}_i$ are the cell averaged value of the state and source vector, and Q_L and Q_R are the solution state on the left and right sides of the cell interface.

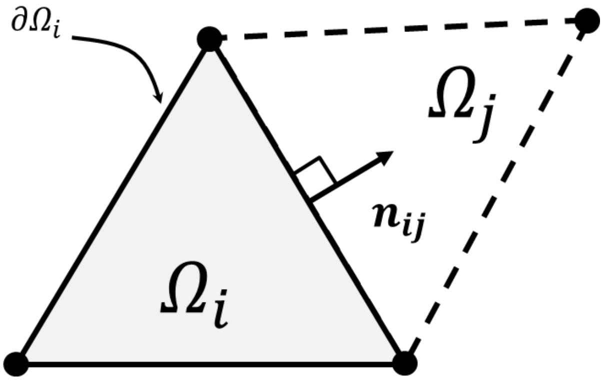

Figure 1: Possible candidate for finite control volume, indicated by Ω_i, its boundary $\partial\Omega_i$, and its outward normal vector n_{ij} associated with face-*j* connecting cell-***i*** and its neighbor cell-***j*.**

3.1 Uniform scheme (P0+P0)

In a uniform first-order scheme, both the solution and its gradient are represented by piecewise constant values within each cell. The flux computation can be expressed as follows,

$$F(Q_L, Q_R; n_{ij}) = \frac{1}{2}\left(F(Q_L) + F(Q_R)\right) - \frac{1}{2}|A|(Q_R - Q_L).$$

Because the cell-averaged value of the solution vector has to be trivially used as the reconstructed solution at the cell-interfaces, the left and right side states are expressed simply as follows,

$$Q_L = \bar{Q}_i \text{ and } Q_R = \bar{Q}_j.$$

The solution accuracy of the hyperbolic system is expected to be first order uniformly, not only for the solution variable itself but also its gradients.

3.2 Hybrid scheme (P0+P1)

The hybrid second-order scheme is composed of a linear representation of the velocity variable (u, v) and piecewise constant representation of the rest variables, i.e. $(p;\ u_x, u_y, v_x, v_y)$. No extra work, such as the least-squares procedure, is performed, like the conventional second-order finite volume schemes; instead, the gradient information about the velocity components are directly recycled from the gradient variables. In this scheme, the flux is evaluated using the linearly reconstructed velocity variables as follows,

$$u_L = \bar{u}_i + u_x|_i \Delta x_{ji} + u_y\big|_i \Delta y_{ji},$$

$$u_R = \bar{u}_j + u_x|_j \Delta x_{ij} + u_y\big|_j \Delta y_{ij},$$

where $(u_x, u_y)_i$ and $(u_x, u_y)_j$ are the gradient variables at two neighbor cells. Note that although the velocities are reconstructed linearly the pressure is piecewise constart which is the same as P0+P0 uniform scheme. Surprisingly this simple treatment improves the accuracy of the pressure as well with no extra effort.

4 Results

Accuracy of the proposed algorithm is presented with the test cases including an exact solution of incompressible Navier-Stokes equations (e.g. Kovasznay flow) and lid-driven cavity problem.

4.1 Kovasznay flow

In this section, an actual flow problem is solved. As the first flow test case, Kovasznay flow[35] is simulated over the rectangular domain of $[-0.5,1] \times [-0.5,1.5]$. The exact solution is expressed as follows:

$$u = 1 - e^{\lambda x} cos(2\pi y),$$

$$v = \frac{1}{2\pi} \lambda e^{\lambda x} sin(2\pi y),$$

$$p = \frac{\left(1 - e^{2\lambda x}\right)}{2},$$

$$\text{where,} \quad \lambda = \frac{Re}{2} - \sqrt{\frac{Re^2}{4} + 4\pi^2}.$$

In order to test the solution behavior under various flow regimes, three levels of Reynolds number are tested with $Re = 40$ and $4{,}000$. At $\mathrm{Re} = 40$, the flow field is similar to that of a wake behind a circular cylinder. As the Reynolds number increases, the flow field becomes more convection dominated and viscous diffusion between the free shear layers becomes thin and weak.
For low Reynolds number case, i.e. Re=40, the uniform and hybrid schemes are compared. As shown in Fig. 2, The uniform scheme shows the first order of accuracy for all solution and gradient variables. The hybird scheme shows two distict trends of convergence depending on mesh levels, as shown in Fig. 3. On coarse meshes, all the solution variables (even including the pressure) shows second order of accuracy but this trends dimishes and becomes to the first order of accuracy on the fine mesh levles.
The improved order of accuracy of the hybrid scheme strengthens for the convection dominated case. For a relatively high Reynolds number case, Re=4,000, the initial second order of accuracy of the solution variables, i.e. (p, u, v), continues down to the finest mesh levels. This results sheds a light that the current simple HINS7 formulation could bring additional order of accuracy not only for the velocity varialbes but also for the pressure varialbe, even without any extra cost.
The qualitative evidence of the current method can be demonstract by the streamlines as shown in Fig. 5. As mesh refines, the dual vortices near the left boundary become evident for both the uniform and hybrid schemes. For the hybrid schemes, the lenght of the vorex is longer than the unform scheme which could the result of less numerical dissipation by the linear reconstruction. Nevertheless, both of the scheme show quite convincing result by recovering the exact solution.
Another evidence of the relative accuracy is presented in Fig. 6. Error norm from the velocity components are displayed and compared for uninform and hybrid schemes. The improvement of the accuracy by the hybrid scheme is clear.

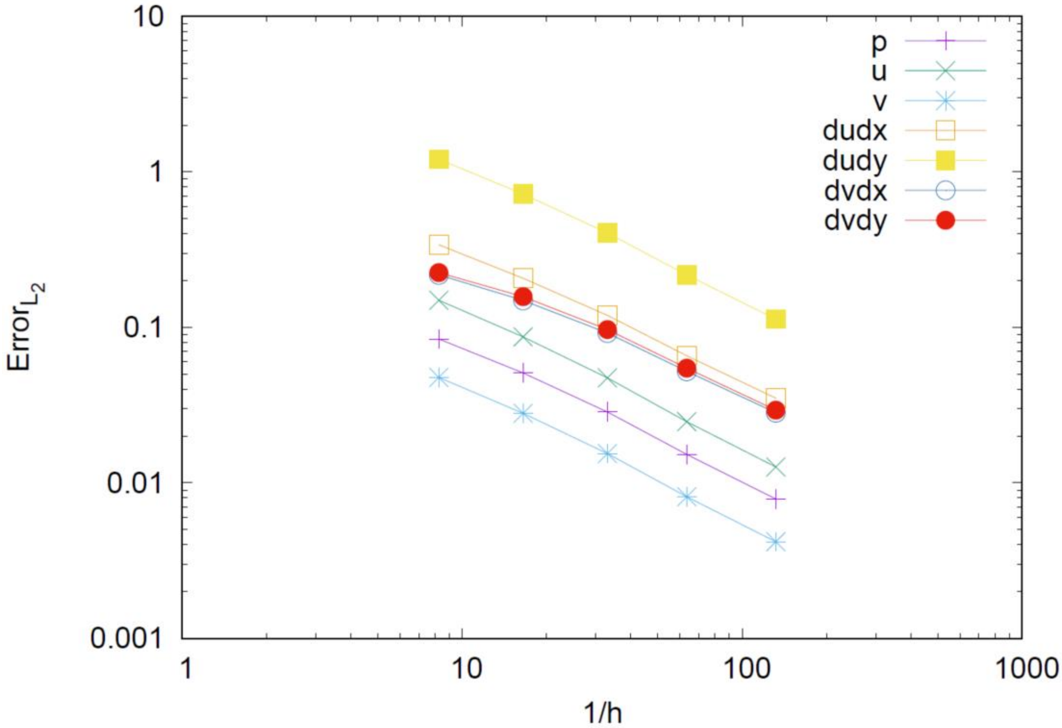

Figure 2: Kovasznay flow with Re=40. Mesh refinement study of uniform P0+P0 scheme. All solution and gradient variables show the expected order of accuracy, which is the first order.

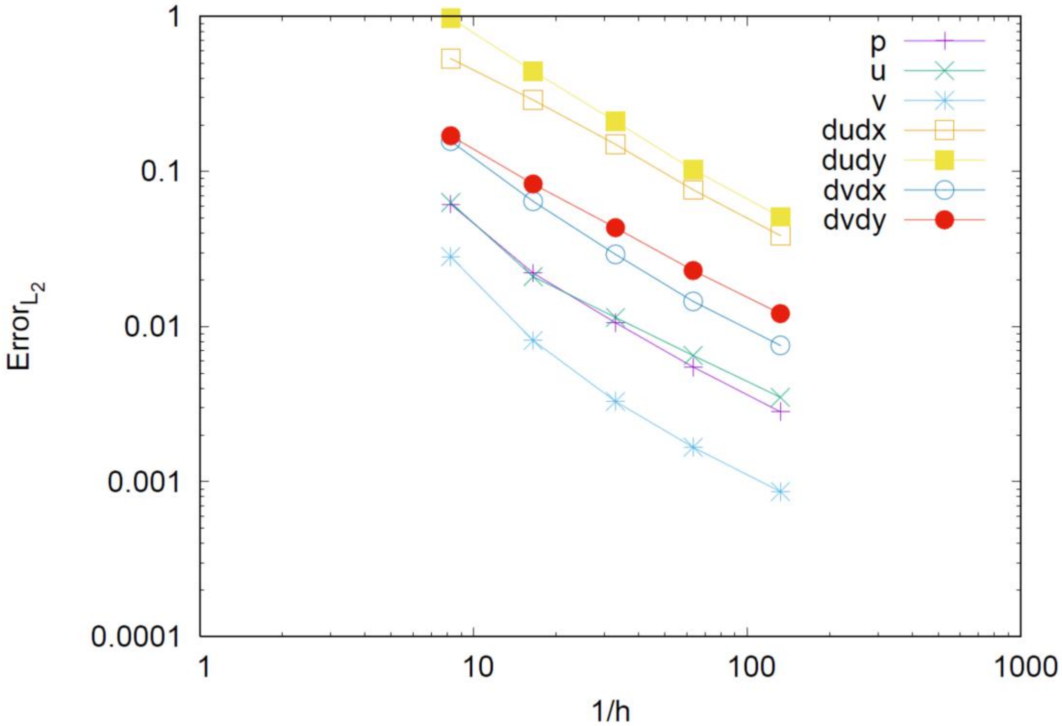

Figure 3: Kovasznay flow with Re=40. Mesh refinement study of uniform P0+P1 scheme. The initial second order accuracy of the solution variables (p, u, v) deteriorates to the first as mesh refines.

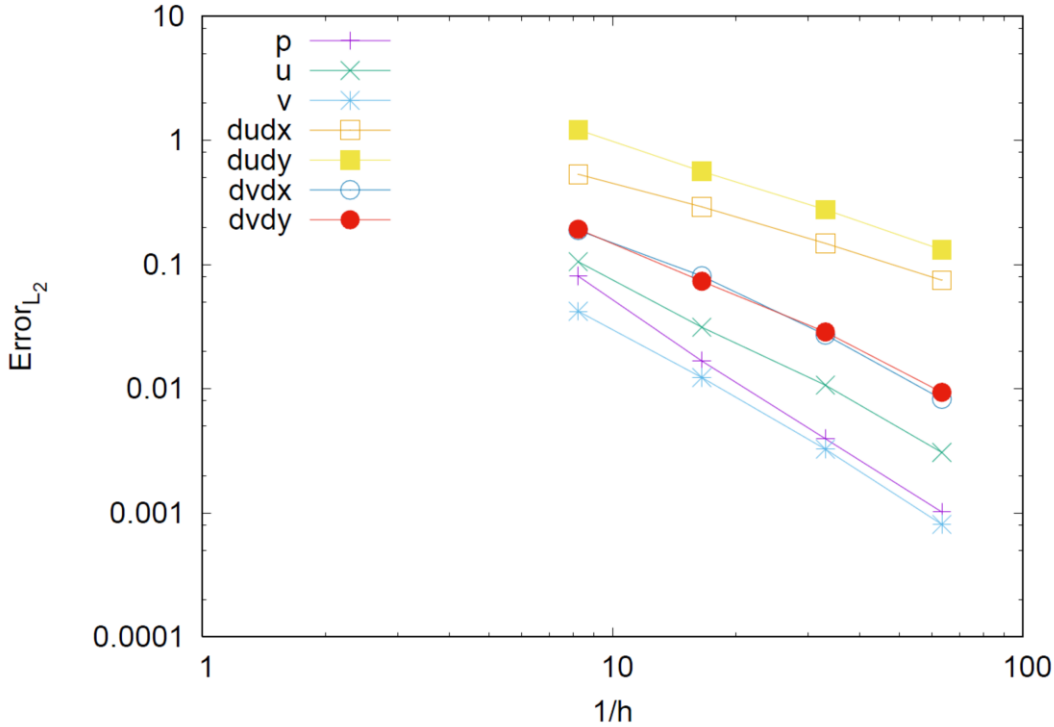

Figure 4: Kovasznay flow with Re=4,000. Mesh refinement study of uniform P0+P1 scheme. The initial second order accuracy of the solution variables (p, u, v) persists even on the finest meshes.

4.2 Driven cavity

In this section, a rather classical test case is simulated for the comparison of solution behavior across different orders of accuracy. The driven cavity problem[8,9] with $\mathrm{Re} = 100$ is simulated and the solution is compared with different order. The no slip condition, i.e., zero velocity for the bottom and side walls and unit velocity for the top wall, is applied, and the Neumann condition is applied for the pressure everywhere.

Unlike the previous test case, no exact solution exists for this case and boundary condition for the gradient variables could be an issue. For this case, the flow is considered as laminar and the boundary layer is considered fully resolved. By this assumption, the velocity gradient becomes linear and also no second derivative curvature effect and this brings us simple zero Neumann boundary condition everywhere.

The results of the uniform and hybrid schemes are displayed in Fig. 7. The equi-spaced vorticity contours are displayed and this indicates the vorticity distribution over the flow domain. As shown in the figure, as mesh refines and also for the hybrid scheme, the asymmetric vorticity distribution becomes more evident.

Fig. 8 shows solution (velocity) distribution along the center lines of the flow field. As mesh refines both of the schemes converges the reference result of Ghia[9]. The hybrid scheme, utilizing linear reconstruction of velocity variables, shows superior results compared to the uniform counterpart.

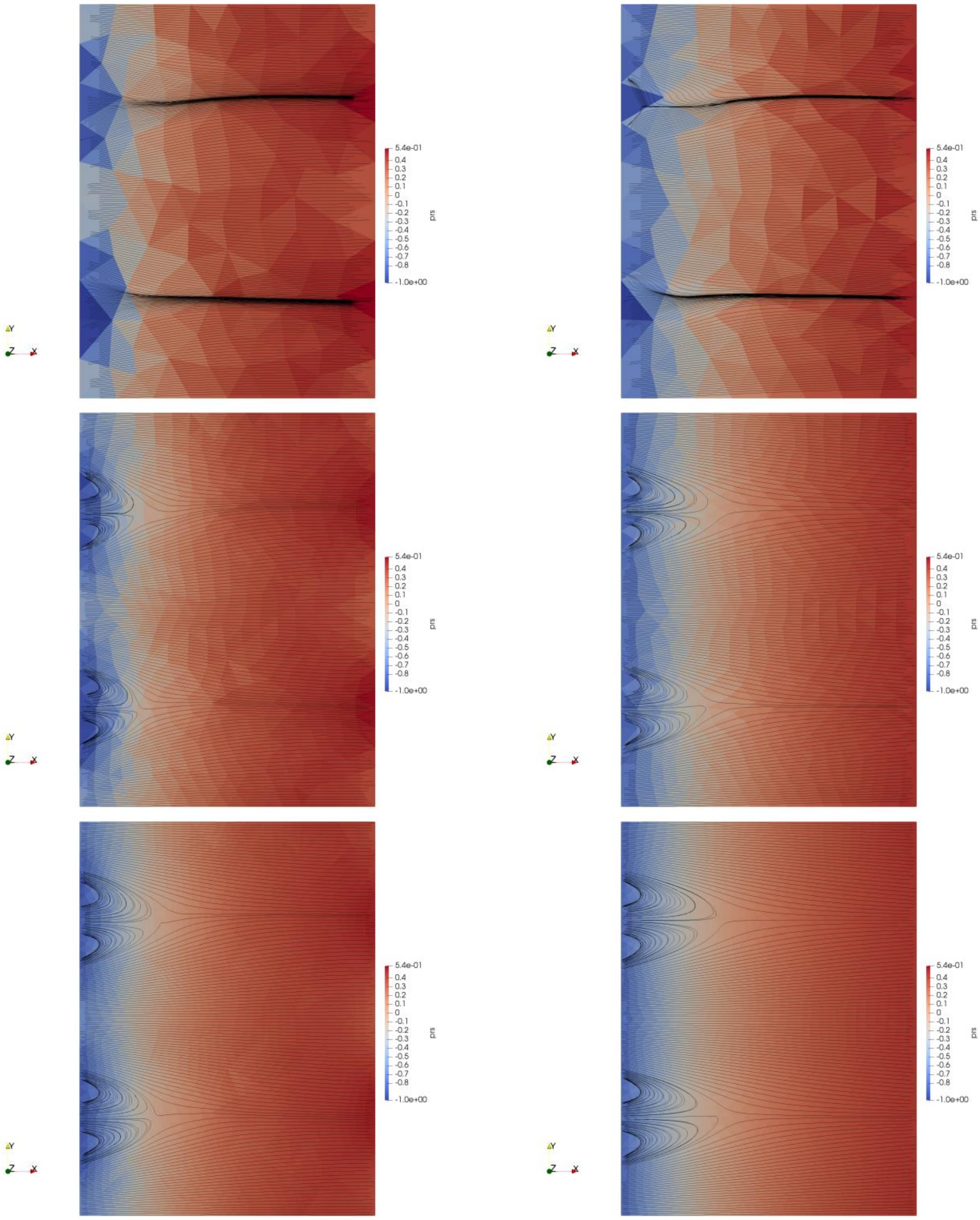

Figure 5: Kovasznay flow with Re=40. Streamlines with background color by pressure. Left column indicates uniform scheme P0+P0 result, and right column from the hybrid P0+P1 scheme. Top, middle, and bottom row corresponds to the coarse, medium and fine meshes, respectively.

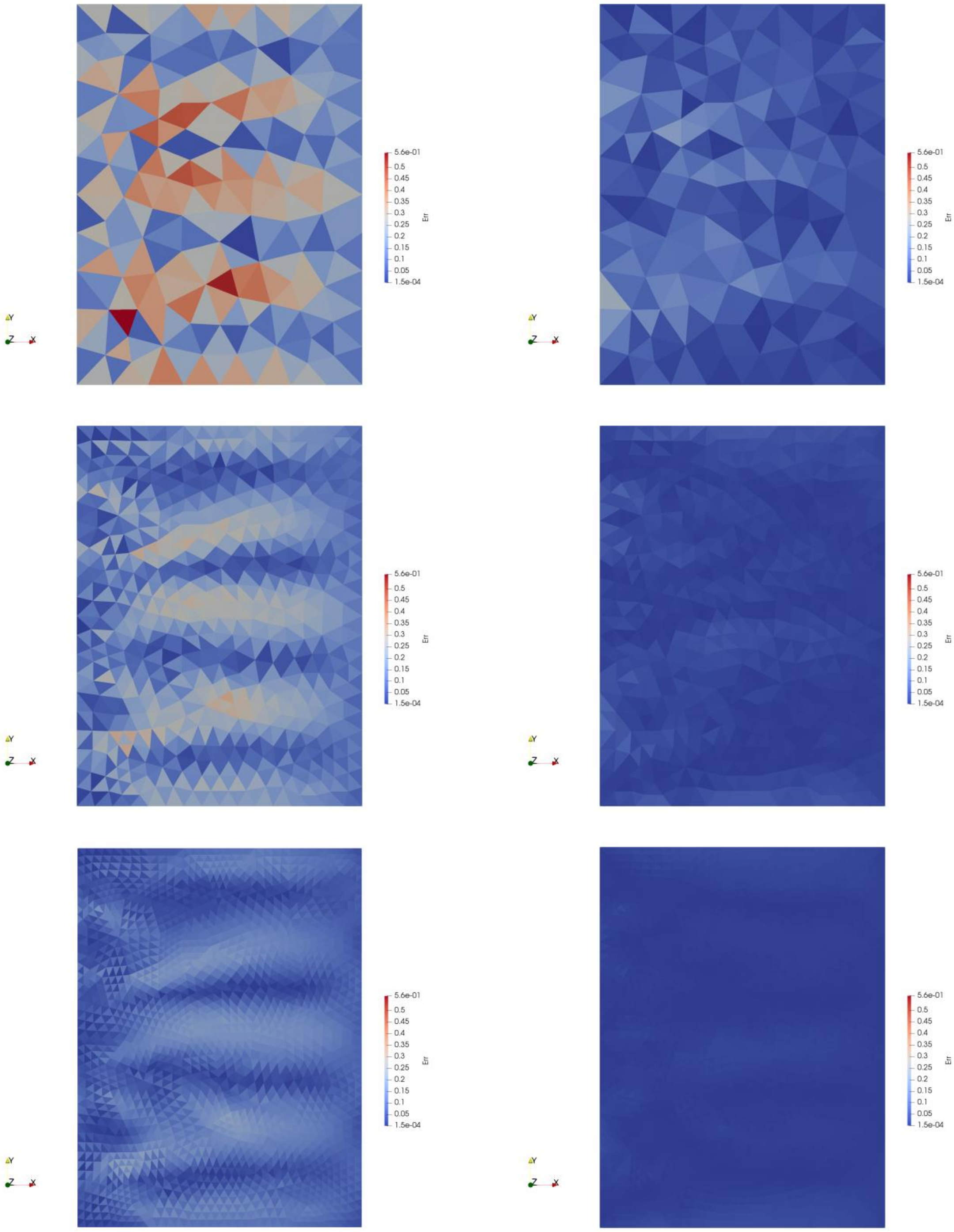

Figure 6: Kovasznay flow with Re=40. Error norm from the velocity components. Left column indicates uniform scheme P0+P0 result, and right column from the hybrid P0+P1 scheme. Top, middle, and bottom row corresponds to the coarse, medium and fine meshes, respectively.

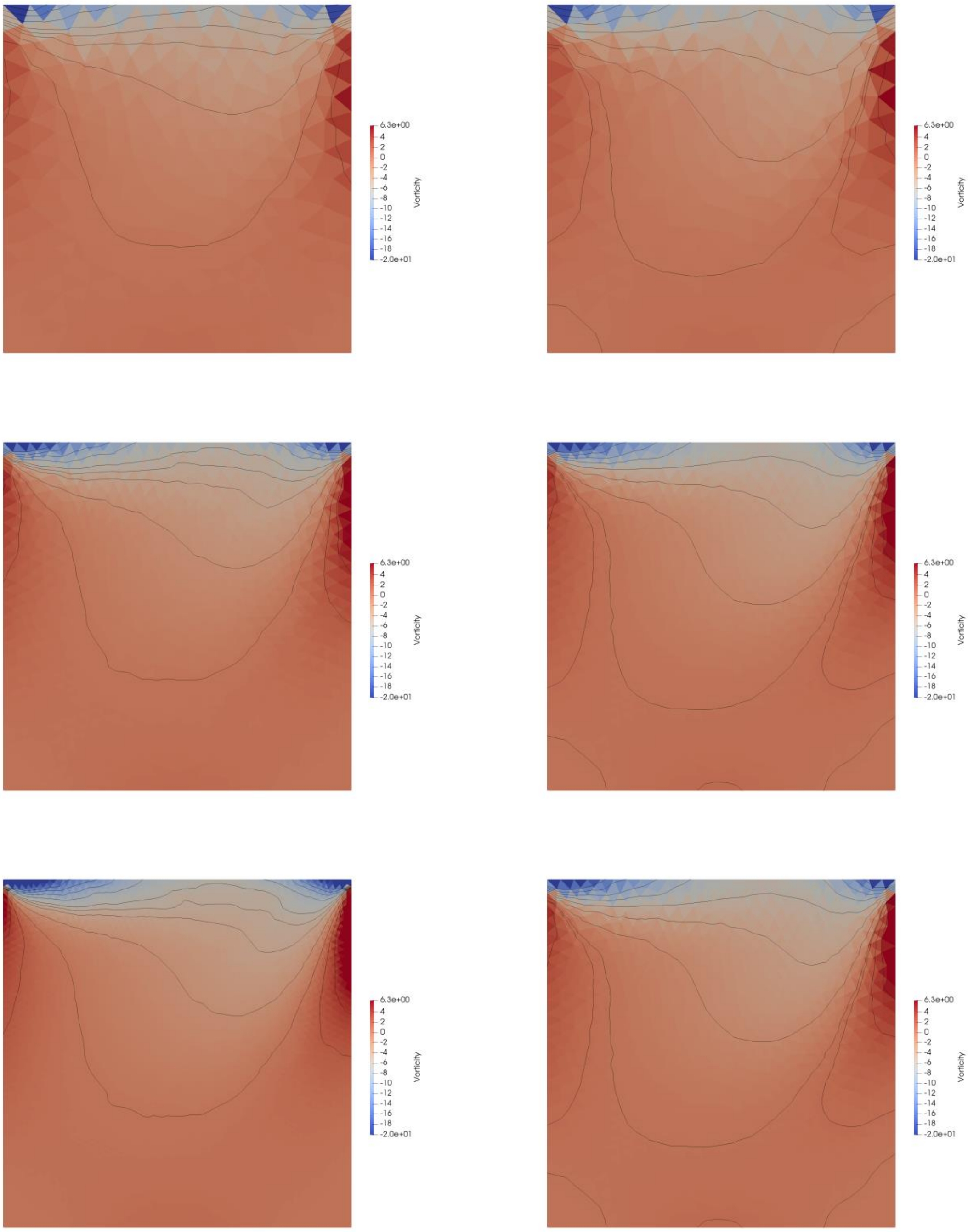

Figure 7: Driven cavity flow with Re=100. Iso-vorticity lines with background color by vorticity. Left column indicates uniform scheme P0+P0 result, and right column from the hybrid P0+P1 scheme. Top, middle, and bottom row corresponds to the coarse, medium and fine meshes, respectively.

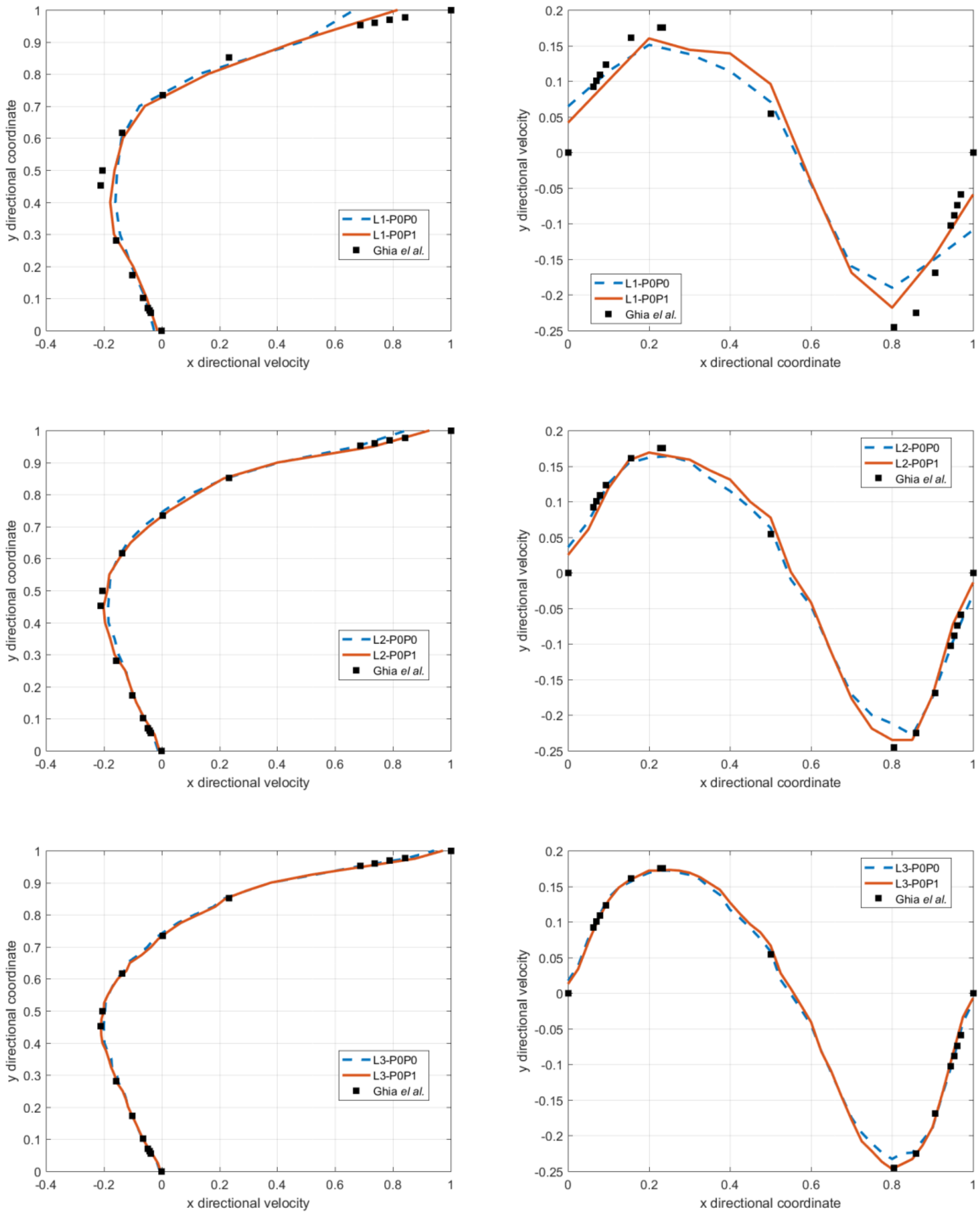

Figure 8: Driven cavity flow with Re=100. Velocity distributions, along the vertical and horizontal half lines. Left column indicates u-velocity distribution along the vertical center lines, and right colum indicates the v-velocity along the horizontal center time. Top, middle, and bottom row corresponds to the coarse(L1), medium(L2) and fine(L3) meshes, respectively.

5 Conclusion

A solution of the hyperbolic method for solving incompressible Navier-Stokes equation is demonstrated. Two different schemes, namely uniform P0+P0 and hybrid P0+P1, are implemented, tested and compared. Superior accuracy of hybrid scheme is observed compared to the uniform scheme, not only for the velocity variables but also for the pressure variables. The current hyperbolic method is very promising for more advanced simulation of incompressible flows.

References

[1] Y. Kallinderis, and H. T. Ahn. Incompressible Navier-Stokes method with general hybrid meshes, J. Comput. Phys., 210:75-105, 2005.

[2] J. Cheng, X. Yang, T. Liu, and H. Luo. A Direct Discontinuous Galerkin method for the compressible Navier-Stokes equations on arbitrary grids. AIAA Paper 2016-1334, 54th AIAA Aerospace Sciences Meeting, 4-8 January, San Diego, California, 2016.

[3] D. Kwak, and C. C. Kiris. Computation of Viscous Incompressible Flows, Springer, 2011.

[4] H. Nishikawa. A First-Order System Approach for Diffusion Equation, I: Second-Order Residual Distribution Schemes. J. Comput. Phys., 227:315-352, 2007.

[5] H. Nishikawa. First, Second, and Third Order Finite-Volume Schemes for Navier-Stokes Equations. AIAA Paper 2014-2091, 7th AIAA Theoretical Fluid Mechanics Conference, Atlanta, 2014.

[6] Y. Nakashima, N. Watanabe, and H. Nishikawa. Hyperbolic Navier-Stokes Solver for Three-Dimensional Flows. AIAA Paper 2016-1101, 54th AIAA Aerospace Sciences Meeting, 4-8 January, San Diego, California, 2016.

[7] E. Lee, H. T. Ahn, and H. Luo. Cell-Centered High-Order Hyperbolic Finite Volume Method for Diffusion Equation on Unstructured Grids. J. Comput. Phys., 355:464-491, 2018.

[8] E. Lee and H.T. Ahn. A reconstruction-based cell-centered high-order finite volume method for incompressible viscous flow simulation on unstructured meshes. Computers & Fluids, 170:187-196, 2018.

[9] U. Ghia, K.N. Ghia, and C.T. Shin. High-re solutions for incompressible flow using the Navier–Stokes equations and an multigrid method. J. Comput. Phys., 48:387-411, 1982.